IEEE/CSC & ESAS EUROPEAN SUPERCONDUCTIVITY NEWS FORUM, No. 22, October/November 2012.
The published version of this preprint appeared in IEEE Transactions on Applied Superconductivity 23, 4700204 (June 2013).

Fast method to quantify the collective magnetization in superconducting magnets

Emmanuele Ravaioli[1,2], Bernhard Auchmann[1], and Arjan P. Verweij[1]

***Abstract*—The magnetization of the superconductor is one of the most important parameters determining the field quality of accelerator magnets. A fast method to quantify the magnetization effect in an entire magnet was developed at CERN based on a voltage-current measurement during a powering cycle. The collective magnetization includes the effect due to hysteresis losses in the magnet superconducting filaments, coupling losses in the magnet conductor, and magnetization of the iron yoke. It is calculated by means of an energy balance between the work done by the power converter and the change of magnetic energy in the system. Also the energy dissipated at any time is calculated. In the magnet test facility at CERN, LHC dipole magnets have been cycled between ±600 A with a ramp-rate of 10 A/s. The magnetization curves deduced from these measurements show a good precision and high reproducibility, mainly due to the high precision of the power converter and the current-measurement system. The results have been compared with numerical simulations performed with the computer code ROXIE. The proposed test method can be applied to any type of magnet, is rather easy and fast, and is therefore interesting for checking the reproducibility of the magnetization among a series production of magnets.**

***Index Terms*—Accelerator magnets, Magnetization, Measurement techniques, Superconducting magnets.**

I. Introduction

THE MAGNETIZATION of the superconductor is one of the most important parameters determining the field quality of accelerator magnets. Usually the magnetization is measured on single superconducting strands or cables [1-5], and the effect on the field quality is then calculated using numerical software [6]. Furthermore, the field quality can be measured using pick-up coils located in the aperture of the magnet [7], and then compared to the expected calculated field.

A fast method to quantify the magnetization effect in an entire magnet was developed at CERN. The voltage across a magnet and the current flowing through it are measured during a current cycle, and the collective magnetization in the magnet is calculated by means of an energy balance between the work done by the power converter and the change of magnetic energy in the system. The collective magnetization includes the effect due to hysteresis losses in the magnet superconducting filaments, inter-filament and inter-strand coupling losses in the magnet conductor, and magnetization of the iron yoke. Also the energy dissipated at any time is calculated. The description of the method is given in Section II.

In order to validate the method and assess its precision, tests have been performed in the magnet test facility at CERN. A LHC twin-aperture dipole magnet has been cycled between ±600 A with a 600 A 10 V four-quadrant power converter. The results have been compared with numerical simulations performed with the computer code ROXIE [6].

The proposed methodology can be applied to any magnet type, and since it is easy and fast it is a useful method for checking the reproducibility of the magnetization effect among a large series of magnets, especially if the existing alternative magnetic measurements are time consuming. The calculated magnetization represents the collective magnetization as a function of the current in the magnet, but it does not give information about the variation of the field quality in different positions of the magnet.

II. Description of the Method

The method relies on the direct measurement of the voltage U across the magnet and of the current I flowing through it during a powering cycle.

A. System Setup

The current in the magnet is cycled by means of a 600 A 10 V four-quadrant power-converter. The measurement system is composed of a high-precision direct current-current transformer (DCCT) [8], a NI-USB-6251-BNC measurement card, and a personal computer.

One channel of the measurement card acquires the differential signal between the voltage taps placed across the magnet, whereas a second channel records the signal measured by the DCCT, corresponding to the current flowing through the magnet. The acquisition frequency was set to 2 kHz.

B. Calculation of the Equivalent Strand Magnetization

For an electromagnetic system the work done by the system dW_{PC} must equal the variation of magnetic energy in the system dE_B [9],

$$dW_{PC} = dE_B = \iiint_V HdB\ dV = \mu_0 \iiint_V HdH\ dV + \mu_0 \iiint_V HdM\ dV\,, \quad [\mathrm{J}] \tag{1}$$

where $B=\mu_0(H+M)$ is the magnetic induction [T], H is the magnetic field [A/m], M is the magnetization [A/m], μ_0 is the vacuum magnetic permeability and equals $4\pi\cdot10^{-7}$ T m/A, and the integrands are integrated over a suitably chosen volume. Given a set of measurement data (U_i, I_i), the work done by the

Manuscript received October 9, 2012.

E. Ravaioli (e-mail: Emmanuele.Ravaioli@cern.ch; phone: 0041-22-7678281) is with the TE department at CERN[1], Switzerland, and with the University of Twente[2], Enschede, The Netherlands.

B. Auchmann and A. P. Verweij are with the TE department at CERN[1], Switzerland.

system, i.e. by the power converter, can be discretized as

$$\Delta W_{PC,i} = UIdt \approx U_i I_i \Delta t, \quad \text{[J]} \quad (2)$$

where the index i refers to the i-th measured point, and Δt is the time between two measured points, i.e. the inverse of the measurement frequency.

The first term on the right side of (1) represents the change of magnetic energy due to a change of the magnetic field. Its change during Δt for a linear inductor can be expressed as

$$\Delta E_{H,i} = \mu_0 \iiint_V H_i \Delta H_i \, dV \approx L_H I_i \Delta I_i, \quad \text{[J]} \quad (3)$$

where L_H is the inductance of the inductor only due to the magnetic field [H]. L_H depends on the geometry of the inductor and can vary with the current due to the saturation of the iron yoke surrounding the magnet. However for small currents it can be approximated as the average value of the differential inductance of the inductor L_d during a powering cycle, since the magnetization-related contributions to L_d during two symmetric positive and negative ramps compensate each other. L_d can be calculated at any time as

$$L_{d,i} = \frac{U}{(dI/dt)_i} \approx \frac{U_i}{(\Delta I/\Delta t)_i} = \frac{U_i}{(I_i - I_{i-1})} \Delta t. \quad \text{[H]} \quad (4)$$

The second term on the right side of (1) represents the energy lost due to magnetization effects. For a superconducting magnet, its variation during Δt is the sum of a contribution due to the hysteretic magnetization change in its superconducting filaments $\Delta E_{M,sc}$, and a contribution due to other magnetization changes $\Delta E_{M,ot}$:

$$\Delta E_{M,i} = \mu_0 \iiint_V H_i \Delta M_i \, dV \approx \mu_0 V_{sc} \overline{H_{sc,i}} \Delta \overline{M_{sc,i}} + \Delta E_{M,ot,i} \quad (5)$$
$$\approx V_{sc} f_{sc} I_i \Delta \overline{M_{sc,i}} + \Delta E_{M,ot,i}, \quad \text{[J]}$$

where $\overline{H_{SC}}$ is the average H inside the superconducting filaments [A/m], $\Delta \overline{M_{SC}}$ the hysteretic magnetization change in its superconducting filaments [A/m], V_{sc} is the volume of superconducting filaments [m^3], and $f_{sc} = \mu_0 \overline{H_{sc}} / I$ can be calculated with numerical simulations [T/A]. The variation $\Delta E_{M,ot}$ is due to the combined effects of the magnetization change in the magnet conductor due to inter-filament and inter-strand coupling-currents [10-11], and of the magnetization change outside the conductor, i.e. mainly in the iron yoke surrounding the magnet. Combining (1-3) and (5) yields

$$\Delta \overline{M_{sc,i}} = \frac{U_i I_i \Delta t - L_H I_i \Delta I_i - \Delta E_{M,ot,i}}{V_{sc} f_{sc} I_i}. \quad \text{[A/m]} \quad (6)$$

Equation (6) expresses the increment of the hysteretic magnetization within the superconducting filaments of the magnet during the time Δt. The average hysteretic magnetization in the filaments of the magnet can be calculated at any time as the sum of all the $\Delta \overline{M_{sc,j}}$ contributions calculated before plus the initial average magnetization $\overline{M_{sc,0}}$:

$$\overline{M_{sc,i}} = \overline{M_{sc,0}} + \sum_{j \le i} \Delta \overline{M_{sc,j}}. \quad \text{[A/m]} \quad (7)$$

Since it is difficult to accurately calculate $\Delta E_{M,ot}$, one can define the collective magnetization

$$M_{col} = \overline{M_{sc}} + E_{M,ot} / (V_{sc} f_{sc} I), \quad \text{[A/m]} \quad (8)$$

where $E_{M,ot}$ is the magnetic energy lost due to magnetization effects other than the hysteresis in the superconducting filaments. Combining (6-8) offers a practical equation for calculating at any time the collective magnetization of a superconducting magnet:

$$M_{col,i} = M_{col,0} + \sum_{j \le i} \frac{U_j \Delta t - L_H \Delta I_j}{V_{sc} f_{sc}}. \quad \text{[A/m]} \quad (9)$$

It is often convenient to define the magnetization per unit volume of conductor, thus replacing V_{sc} in (9) with the total volume of the conductor V_c. Equation (9) contains only measured values of U, I, and Δt, the parameters L_H, f_{sc}, and V_{sc}, depending on geometric properties of the magnet and usually well known, and $M_{col,0}$. The latter is zero for the first magnetization cycle performed after the cooling down of the magnet. For subsequent cycles, it can be taken as the last calculated value of M_{col} in the previous cycle, or estimated considering the magnetic history of the magnet.

III. Application of the Method

A. Test Magnet

In order to validate the technique presented in Section II, voltage-current measurements were performed at a temperature of 1.9 K in the CERN magnet test facility. The measured magnet (MB1089) is a LHC twin-aperture main dipole magnet [12], with V_c=0.0997 m^3 and V_{sc}=0.0354 m^3. It is composed of two different Nb-Ti cable types: in the inner, higher field region the cables are thicker and their superconducting filaments have a diameter d_f of 7 µm; in the outer, lower field region d_f=6 µm. f_{sc} was evaluated with numerical simulations and equals 455 µT/A. for the tested magnet L_H equals 98.1 mH, calculated as the average L_d within a ±600 A powering cycle (see Section II.b).

B. Calculated Collective Magnetization

The test presented in this paper featured two powering cycles with constant ramp-rate. Fig. 1 shows the U and I signals recorded during Cycle 1 and 2, together with the calculated ramp-rate dI/dt. It can be observed that during the ramps dI/dt remained constant whereas the voltage across the magnet varied. This is due to the fact that the differential inductance is not constant throughout the cycle.

FIG. 1 HERE

The calculated differential inductance as a function of the magnet current is shown in Fig. 2. The initial value of L_d was less than 85% of L_H. This is due to the residual positive magnetization within the magnet, which gave a negative contribution to L_d. The two cycles presented in this paper were preceded by a negative ramp of the current, thus initially they both present $L_d < L_H$. This phenomenon is the reason why the inductance of the LHC main dipole magnets measured with a frequency-sweep at very low current was often found to be smaller than the expected value [13].

FIG. 2 HERE

Fig. 3 shows the calculated collective magnetization within the magnet conductor as a function of the current I during Cycle 1 and 2. The average hysteretic magnetization within the magnet superconducting strands $M_{sc,ROXIE}$, modeled with a numerical simulation carried out using the program ROXIE and averaged over the magnet strands, is presented as well. Considering (8), one can see that the difference M_{col}-$M_{sc,ROXIE}$ gives an indication of the value of $E_{M,ot}$. This value is affected by a large number of errors though, coming from the voltage-current measurement error, the inaccuracy of the ROXIE magnetization model at very low fields, end effects in the two magnet extremities, and the imprecision in the calculation of L_H, f_{sc}, and V_c.

The magnetization within the conductor in Cycle 1 and 2 is mainly due to hysteretic effects. In fact, the contributions to the strand magnetization due to inter-filament and inter-strand coupling-losses M_f and M_s were estimated to be very small as compared to the hysteretic magnetization. In fact, from [10]

$$M_f \approx \left(\frac{l_w}{2\pi}\right)^2 \frac{1}{\rho_{eff}} \frac{dB}{dt} \approx \left(\frac{l_w}{2\pi}\right)^2 \frac{1}{\rho_t} f_{sc} \frac{dI}{dt}, \quad \text{[A/m]} \qquad (10)$$

where l_w is the cable twist-pitch [m], and ρ_t its effective transverse resistivity [Ωm]; and from [11]

$$M_s \approx 8.49 \cdot 10^{-3} \frac{l_w \left(N_s^2 - N_s\right)}{R_c} \frac{w}{h} \frac{dB_\perp}{dt}, \quad \text{[A/m]} \qquad (11)$$

where N_s is the number of strands in the cable, w and h the broad and narrow dimensions of its cross-section [m], R_c the contact resistance between two strands [Ω], and $B_\perp$ the magnetic induction perpendicular to the cable broad face [T]. During Cycle 1 and 2 dI/dt =±10 A/s and $\mu_0 M_f$ and $\mu_0 M_s$ are estimated to be smaller than ±0.1 mT both in the inner and outer strands.

The average magnetization in the conductor is thus the result of the hysteretic magnetization among strands which behave differently. In fact, in the strands located in high-field regions of the magnet the magnetic field changes more quickly than in those located in the low-field regions. Besides, since the critical current density in the superconducting strands J_C is higher at lower field, the penetration field H_P=$J_C(B)d_f/\pi$ is larger in the low-field strands. When in a strand H>H_P, the magnetic field fully penetrates its filaments and M_{sc} in the strand reaches the saturation value defined by [10]

$$M_{sat} = \pm \frac{2\lambda d_f J_C(B)}{3\pi}, \quad \text{[A/m]} \qquad (12)$$

where λ is the fraction of superconductor in the magnet strands. Saturation curves for the two strand types in the magnet calculated with the $J_C(B)$ fit proposed in [14] are shown in Fig. 4.

At the beginning of Cycle 1 most high-field strands were fully magnetized due to the magnetic field remaining from a precedent magnetization cycle, whereas most low-field strands had a positive but unsaturated magnetization.

As the current increased, the magnetic field in the strands increased and the magnetization-change was negative in order to oppose to the field-change. The strands saturated when their magnetic field reached their respective -H_p. Assuming H≈H_p in all the strands at the beginning of the cycle, one can assume that any strand saturated after a field-change of about $2H_P$, and then estimate the number of saturated strands during the cycle by calculating H and H_p of each strand. About 30% of the strands saturated below 200 A, 65% below 400 A, and 85% below the maximum current of the cycle 600 A. These figures should be increased since some strands started the cycle with H<H_p and needed a smaller field-change to saturate. The average magnetization in the strands at 600 A approached the value of M_{sat}.

During the second half of Cycle 1, the current decreased and most of the high-field strands quickly re-saturated to a positive value of magnetization. However, in the low-field strands H_P was larger, and the field-change smaller and too little for fully saturating the filaments. At the end of Cycle 1, when the current reached zero, about 60% of the strands were saturated.

Most of the low-field strands that did not reach saturation during the negative ramp of Cycle 1 saturated when the field was further decreased, at the start of Cycle 2. This is the reason why the calculated magnetization curve has a positive peak at a negative current instead of at zero. When the current reached the minimum value -600 A, nearly all the strands were saturated.

The behavior of the strand magnetization during the positive ramp from -600 to 600 A was similar to that during the negative ramp: the high-field strands saturated more quickly than the low-field ones, about 60% of the strands saturated before reaching positive current, and at 600 A nearly all the strands had reached saturation.

During the final current ramp back to zero which concluded Cycle 2, the magnetization effects closely replicated those occurred during the ramp 600-0 A of Cycle 1.

It is likely that the area of the loop defined by the evolution of the quantity M_{col}-$M_{sc,ROXIE}$, related to $E_{M,ot}$, during Cycle 2 is linked to a hysteresis loop due to magnetization of the iron yoke surrounding the magnet.

The explanation for the two peaks of M_{col}-$M_{sc,ROXIE}$ at low current (|I|<150 A) seems to be related to the ROXIE magnetization model which is less reliable at very low fields.

FIG. 3 HERE

Fig. 4 shows W_{PC}, E_H, and E_M, defined as the discretized integrals of the quantities introduced in (2), (3), and (5) respectively. For each complete magnetization cycle, E_H is zero and E_M=W_{PC} is proportional to the area enclosed within its magnetization loop (see (5) and Fig. 3).

The energy lost in identical powering cycles was calculated with a precision of 0.5%. The very high reproducibility of this loss is mainly due to the high precision of the power converter and of the DCCT.

FIG. 4 HERE

IV. Conclusion

A fast method to quantify the magnetization effect in an entire magnet was developed at CERN based on the

The published version of this preprint appeared in IEEE Transactions on Applied Superconductivity 23, 4700204 (June 2013).

measurement of the voltage across the magnet and its current during a powering cycle. The calculated magnetization represents the collective effect of the magnetization in the superconducting filaments of the magnet, and of the magnetization of the iron yoke. At low ramp-rate the magnetization in the conductor is mostly due to the hysteresis in the superconducting filaments of the magnet since the contributions due to inter-filament and inter-strand coupling losses are limited.

The collective magnetization is calculated by means of an energy balance between the work done by the power converter and the change of magnetic energy in the system.

The difference between the calculated collective magnetization and the magnetization in the superconducting strands simulated with the numerical program ROXIE gives an indication of the energy lost due to magnetization effects other than the hysteresis in the superconducting filaments.

The energy lost due to the magnetization effect was measured in independent cycles with a precision of 0.5%.

The proposed method shows good precision and very high reproducibility, is fast and fairly easy to apply, and can be performed on any magnet type. Good-precision DCCT and power converters are needed for obtaining such high precision.

This method can be used for checking the reproducibility of the magnetization effect among a large series of magnets, and thus detecting possible outliers. It is especially useful to assess the magnetization effect as a function of the current in a magnet without a time-consuming measurement of field error with rotating or fixed coils.

ACKNOWLEDGMENT

The authors want to thank Miguel Cerqueira Bastos, Guy Deferne, Christian Giloux, Bernard Dubois, Emmanuel Garde, and Hugues Thiesen for their help during the powering tests.

REFERENCES

[1] S. Le Naour, et al., "Magnetization measurements on LHC superconducting strands," *IEEE Trans. Appl. Supercond.*, pt. 2, vol. 9, no. 2, pp. 1763-1766, 1999.

[2] S. Le Naour, R. Wolf, J. Billan, and J. Genest, "Test station for magnetization measurements on large quantities of superconducting strands," *IEEE Trans. Appl. Superconduct.*, pt. 3, vol. 11, no. 1, pp. 3086-3089, 2001.

[3] R. Wolf and S. Le Naour, "The expected persistent current field errors in the LHC main dipole and quadrupole," CERN, Geneva, Switzerland, LHC Project Note 230, 2000.

[4] B. Bellesia, et al., "Spread in dipole cable magnetization and consequences on the Spread of DC persistent currents in the main dipole of the Large Hadron Collider," LHC Project Note 365, 2004.

[5] B. Bellesia, et al., "Trends in cable magnetization and persistent currents during the production of the main dipoles of the Large Hadron Collider," *IEEE Trans. Appl. Supercond.*, vol. 15, no. 2, pp. 1213-1216, 2005.

[6] S. Russenchuck, "ROXIE, Routine for the optimization of magnet Xsections, inverse field computation and coil end design", Proceedings of the First International ROXIE Workshop, CERN, Geneva, March 1998.

[7] L. Walckiers, "Magnetic measurement with coils and wires," CERN Accelerator School CAS 2009: Specialised Course on Magnets, Bruges, June 2009.

[8] G. Hudson, K. Bouwknegt, "4-13 kA DC current transducers enabling accurate in-situ calibration for a new particle accelerator project, LHC," *Power Electronics and Applications*, *2005 European Conference on*.

[9] J. R. Reitz, F. J. Milford, R. W. Christy, "Foundations of electromagnetic theory," Addison-Wesley Pub. Co., USA, 1960.

[10] M. Wilson, "Superconducting magnets," Clarendon Press, Oxford, GB, 1983.

[11] A. Verweij, "Electrodynamics of superconducting cables in accelerator magnets," chapter 4, PhD thesis University of Twente, The Netherlands, 1995.

[12] "LHC design report", CERN-2004-003 (2004).

[13] K. Dahlerup-Petersen, F. Schmidt, "Impedance measurements and modeling of the ten meter prototype LHC dipole magnet," LHC Project Note 11, 1995.

[14] A. Verweij, "CUDI: Users manual," CERN, 2007.

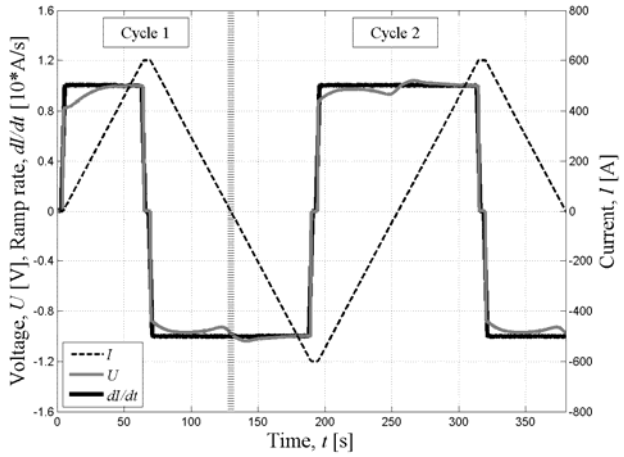

Fig. 1. Measured voltage across the magnet U and current I, and calculated ramp-rate, dI/dt (Cycles 1 and 2).

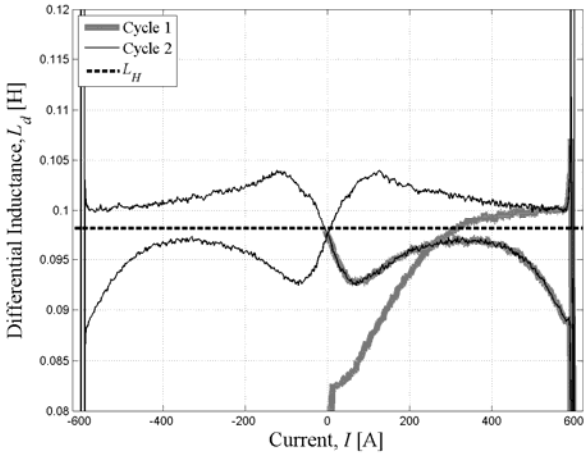

Fig. 2. Calculated differential inductance, L_d (Cycles 1 and 2).

The published version of this preprint appeared in IEEE Transactions on Applied Superconductivity 23, 4700204 (June 2013).

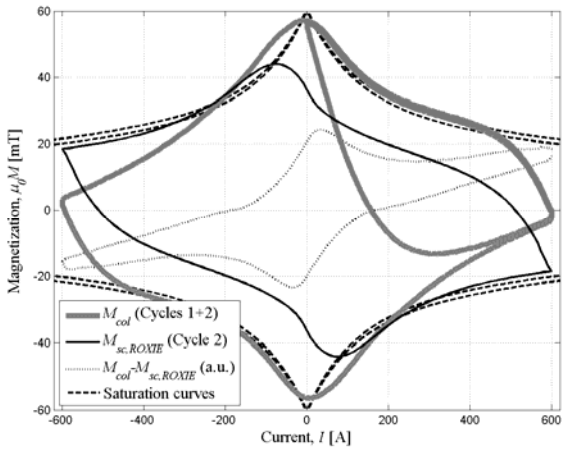

Fig. 3. Calculated collective magnetization, M_{col} (Cycles 1 and 2), ROXIE-simulated average strand magnetization $M_{sc,ROXIE}$, their difference (in arbitrary units), and saturation curves M_{sat} for the inner and outer strands.

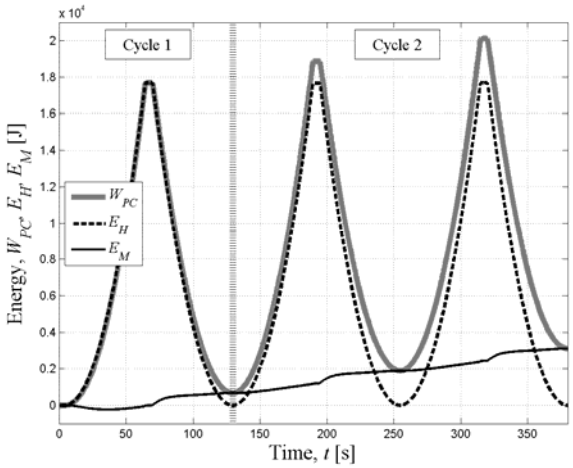

Fig. 4. Calculated work done by the system, W_{PC}, magnetic energy due to a change of H, E_H, and magnetic energy due to a change of M, E_M (Cycles 1 and 2).